

Effects of an electronic topological transition for anisotropic low-dimensional superconductors

G. G. N. Angilella,¹ E. Piegari,^{2,3} and A. A. Varlamov⁴

¹*Dipartimento di Fisica e Astronomia, Università di Catania, and Istituto Nazionale per la Fisica della Materia, UdR di Catania, Corso Italia, 57, I-95129 Catania, Italy*

²*DMFCL, Università di Catania, Viale A. Doria, 6, I-95125 Catania, Italy*

³*Istituto Nazionale per la Fisica della Materia, UdR di Firenze, Via G. Sansone, 1, I-50019 Sesto Fiorentino (FI), Italy*

⁴*Istituto Nazionale per la Fisica della Materia, UdR di Tor Vergata,*

DSTFE, Università di Roma "Tor Vergata," Via di Tor Vergata, 110, I-00133 Roma, Italy

(Received 10 May 2001; revised manuscript received 20 December 2001; published 20 June 2002)

We study the superconducting properties of a two-dimensional superconductor in the proximity to an electronic topological transition (ETT). In contrast to the three-dimensional (3D) case, we find that the superconducting gap at $T=0$, the critical temperature T_c , and the impurity scattering rate are characterized by a nonmonotonic behavior, with maxima occurring close to the ETT. We derive analytical expressions for the value of such maxima both in the s -wave and in the d -wave cases. Such expressions are in good qualitative agreement with the phenomenological trend recently observed for T_c^{\max} as a function of the hopping ratio t'/t across several cuprate compounds. We further analyze the effect of an ETT on the Ginzburg-Landau stiffness η . Instead of vanishing at the ETT, as could be expected, thus giving rise to an increase of the fluctuation effects, in the case of momentum-independent electron-electron interaction, we find $\eta \neq 0$, as a result of an integration over the whole Fermi surface.

DOI: 10.1103/PhysRevB.66.014501

PACS number(s): 74.20.-z, 74.62.-c, 74.40.+k

I. INTRODUCTION

The unconventional properties of the normal and superconducting states of several low-dimensional novel electronic materials is a source of continuous interest and research. Such materials include the high- T_c cuprate superconductors (HTSC's),¹ as well as some organic superconductors based on doped BEDT-TTF layers, and the ruthenates. In these materials, the interplay between their reduced dimensionality and the strength of the effective electron-electron interaction is believed to be the key for the elusive nature of their normal state, as well as for the anisotropic gap characterizing their superconducting state.

A feature common to almost all the material classes listed above is a quasi-2D dispersion relation, arising from their layered structure and stabilized by the tendency to confined coherence within layers, due to strong correlations.² Indeed, flat bands have been observed in nearly all hole- and electron-doped superconductors,³ in the κ phase of BEDT-TTF organic superconductors,⁴ as well as in the noncuprate layered superconductor Sr_2RuO_4 (Ref. 5). Clear evidence for a 2D Fermi surface changing topology as a function of doping has been recently provided by ARPES measurements in LSCO.⁶ In particular, the role of the proximity to an electronic topological transition in establishing the unconventional properties especially of the cuprates has been very early emphasized (see Ref. 7 for a review). Therefore, in the following we will be mainly concerned with the case of the high- T_c cuprates.⁸

The term electronic topological transition has been proposed in order to describe the phenomena related to a change of the connectivity number of the components of the Fermi surface (FS).⁹ Such a transition can be driven by several causes such as isotropic pressure, anisotropic deformation, and the introduction of isovalent impurities. All these influ-

ences can be parametrized by their effect on the chemical potential μ passing through the critical value ε_c , corresponding to the transition point. Indeed, such a critical point can be well defined only in a pure metal at $T=0$ where a true phase transition of order $2\frac{1}{2}$ occurs,¹⁰ according to Ehrenfest classification. Typical manifestations of an ETT consist in cusplike anomalies of physical quantities such as the specific heat,¹¹ the density of states (DOS), and the conductivity, as well as in the appearance of asymmetric singularities of the thermal expansion coefficient and thermoelectric power in the dependence of all these quantities on $z = \mu - \varepsilon_c$. A non-zero temperature or the presence of electron scattering results in the smearing of these anomalies and, strictly speaking, in washing out the notion of a $2\frac{1}{2}$ -order phase transition itself. Moreover, the occurrence of an ETT can be masked by an intervening structural transition, as could be induced by external pressure. The effects of an ETT on the properties of metals and alloys have been thoroughly investigated as well.^{9,12,13}

In lower dimensional metallic systems, an ETT is characterized by yet stronger anomalies. In particular, the DOS of a 2D metal increases logarithmically near an ETT, instead of displaying a square-root cusp, as in the 3D case.¹⁴ Therefore, it has been suggested that an ETT may be a clue for the understanding of the anomalous superconducting state of the high- T_c cuprates.⁷ In particular, it is well known that the presence of an ETT in the spectrum of a 2D superconductor induces a nonmonotonic dependence of the critical temperature on doping or applied pressure,^{7,15} in qualitative agreement with the available experimental results.^{16,17} This has to be contrasted with the 3D case, where an ETT only gives rise to a steplike behavior in the z dependence of T_c .¹⁸

Moreover, it has been proposed that the proximity to an ETT may be the origin of the unconventional normal state of

the HTSC. In particular, a marginal Fermi liquid^{19–22} or a non-Fermi-liquid²³ behavior can be naturally derived for a 2D electron system near a van Hove singularity. More generally, it has been argued that the anomalous finite-temperature phenomenology of the cuprates stems from the competition of several broken-symmetry states intervening near one and the same quantum critical point (QCP).^{24,25} Recently, Onufrieva *et al.*^{26,27} showed that an ETT occurring in a 2D square lattice with hopping beyond nearest neighbors is a QCP, with two aspects of criticality: the first is related to the singular behavior of the thermodynamic properties (van Hove singularity), while the second is related to the existence of the critical line $T=0$, $z>0$ of static Kohn singularities.^{26,27} The proximity to an ETT may be characterized by spin density wave (SDW), charge density wave (CDW), and d -wave superconducting (dSC) instabilities, depending on the appropriate interaction channels included in the analysis. Onufrieva *et al.* argued that SDW fluctuations dominate in the case of the high- T_c cuprates.²⁸ On the other hand, recent studies focussed on the competition between AFM and AFM-mediated d -wave pairing via a diagrammatic approach,²⁹ among dSC, AFM, and π -triplet pairing at a mean field level in the presence of backward scattering,³⁰ among dSC, AFM, and CDW within the renormalization group (RG) approach,^{31–33} among dSC, AFM, and FM within the RG and the parquet approaches,³⁴ or between dSC and an excitonic ordered state.³⁵ More recently, it has been shown³⁶ that elastic umklapp scattering near a van Hove singularity may give rise to an RVB-like, insulating spin liquid state,³⁷ which exhibits both d -wave superconducting and AFM correlations, without being characterized by true symmetry breaking, as is typical of a quantum ordered state. The competition between superconductivity and various kinds of density waves in several low-dimensional electron systems in the presence of a van Hove singularity has been reviewed both from the experimental and the theoretical point of view in Ref. 38.

In this paper, we will concentrate on a single superconducting instability (towards either an s -wave or a d -wave superconducting state), in the weak coupling limit, thus neglecting altogether any other competing ordered phase, for a 2D electron system near an ETT. This is of course justified only if all other instabilities are characterized by weaker couplings, which may not be the case for the cuprates. However, such an approximation will enable us to derive an analytical expression for the maximum gap Δ_0 near the ETT as a function of the band details. Such results are in good qualitative agreement with recent studies of T_c in the cuprates correlated with material dependent properties, such as the ratio of next-nearest- to nearest-neighbor hopping.³⁹

We will also study the effect of an ETT on the Ginzburg-Landau stiffness $\eta \propto Gi^{-1}$, where Gi is the Ginzburg-Levanyuk parameter, which characterizes the manifestation range of fluctuations near T_c (Ref. 40). In the case of an isotropic FS, η is proportional to the square of the Fermi velocity. In the vicinity of an ETT, due to the presence of “slow” electrons near the saddle point in the electronic spectrum, one may expect an increase of fluctuations. However, we will show that, in the case of a momentum-independent

electron-electron interaction, all electronic states on the FS participate in establishing the superconducting correlations. Such correlations give rise to a superconducting stiffness, whose value is of the same order of magnitude of the result obtained for an isotropic electronic spectrum,⁴¹ to the lowest order in z/E_F .

The paper is organized as follows. In Sec. II, we introduce a dispersion relation beyond nearest neighbors for an electron system in a 2D square lattice, as is typical for the cuprates, and discuss its corresponding singular DOS. In Sec. III, we study the superconducting gap Δ_0 at $T=0$ as a function of the critical parameter z , in the case of s - and d -wave pairing. In Sec. IV, we discuss the effect of impurities on the normal state DOS and show that the proximity to an ETT gives rise to a nonmonotonic z dependence of the renormalized quasiparticle inverse lifetime τ^{-1} . In Sec. V, we calculate the Cooper pair propagator near an ETT, and discuss the effects of an ETT on the superconducting fluctuations. We eventually summarize in Sec. VI.

II. THE MODEL

Detailed band structure calculations within the local-density approximation (LDA),⁴² as well as ARPES experiments,⁴³ show that a realistic tight-binding approximation for the band dispersion of most quasi-2D cuprates has to be expanded at least up to next-nearest-neighbors hopping. We then assume the following rigid band dispersion relation for a tetragonal lattice:

$$\xi_{\mathbf{k}} = \varepsilon_{\mathbf{k}} - \mu = -2t(\cos k_x + \cos k_y) + 4t' \cos k_x \cos k_y - \mu, \quad (1)$$

where μ denotes the chemical potential, and the components of the wave vector \mathbf{k} are measured in units of the inverse lattice spacing. A nonzero value of the hopping ratio $r = t'/t$, measuring the ratio of next-to-nearest- vs nearest-neighbors hopping, slightly modulates the actual shape of the Fermi line $\xi_{\mathbf{k}}=0$, and in particular destroys perfect nesting at $\mu=0$ as well as electron-hole symmetry (Fig. 1). In order to have a flat minimum in $\xi_{\mathbf{k}}$ around the Γ point, as is observed experimentally for the majority of the cuprates,^{44–46} the condition $0 < r < \frac{1}{2}$ must be fulfilled. The role of an extended saddle point in stabilizing superconductivity against other possible low-energy instabilities has been established within the renormalization group (RG) approach in the weak-coupling limit.³³ Moreover, it has been shown that an increase of r in the mentioned range correlates with an increase of the maximum T_c across different classes of cuprate superconductors.³⁹ However, changes of the *shape* of the FS resulting from screening effects can also correlate with changes in the superconducting properties in an indirect way. Indeed, a deformation of the FS also induces a change of the phase space effectively probed by the electron-electron interaction.⁴⁷ This is particularly relevant for several models proposed for the HTSC, characterized by effective interactions peaked at $X=(0,\pi)$, namely, exactly where the Fermi line is most sensible to a change in the hopping range r . Possible realizations of such a strongly anisotropic \mathbf{k} -dependent potential include the interaction mediated by

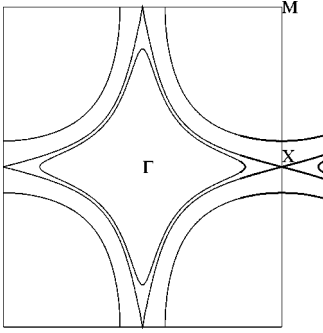


FIG. 1. Fermi line $\xi_{\mathbf{k}}=0$, Eq. (1), for a value of the hopping ratio $r=0.45$. As the chemical potential varies from the bottom to the top of the band, the Fermi line changes topology, evolving from a closed contour around the Γ point, to a contour, whose continuation in the higher order Brillouin zones closes around $M=(\pi, \pi)$. The change of topology (ETT) occurs when the Fermi line touches the zone border, i.e., at $X=(\pi, 0)$, and symmetry related points. The thicker solid lines evidence the hyperbolalike shape of the Fermi line, Eq. (2), around X .

antiferromagnetic spin fluctuation⁴⁸ or by quasicritical stripe fluctuations, due to the proximity to a QCP near optimal doping at $T=0$ (Refs. 49–51), as well as electron-electron interactions enhanced by interlayer pair-tunneling (ILT).^{52,53}

As the chemical potential μ in Eq. (1) varies from the bottom, $\varepsilon_{\perp} = -4t(1-r)$, to the top of the band, $\varepsilon_{\top} = 4t(1+r)$, the Fermi line $\xi_{\mathbf{k}}=0$ evolves from an electronlike contour, closed around the Γ point, to a holelike contour, whose continuation into higher order Brillouin zones closes around the $M=(\pi, \pi)$ point. In doing so, an ETT is passed exactly at $\mu = \varepsilon_c = -4t'$, where the Fermi line touches the zone boundaries, and assumes the asteroidlike shape depicted in Fig. 1. It has been shown that such a critical value for the Fermi energy is stable against the RG flow for any repulsive electron-electron interaction.^{54,55} Such a result has been recently confirmed also when self-energy effects to the quasiparticle dispersion relation are included, thus demonstrating that the pinning of the Fermi surface to a van Hove singularity can actually take place for a rather wide range of hole concentration.⁵⁶ The condition $\mu = \varepsilon_c$ corresponds to having a saddle point at $X=(\pi, 0)$ in the single-particle dispersion relation $\varepsilon_{\mathbf{k}}$, which, for small wave vector displacements from X and symmetry related points, can be expanded as

$$\varepsilon_{\mathbf{k}} - \varepsilon_c \sim \frac{p_1^2}{2m_1} - \frac{p_2^2}{2m_2} \equiv \epsilon_{\mathbf{p}}, \quad (2)$$

where $p_1 = k_x$, $p_2 = k_y - \pi$, and $m_{1,2} = [2t(1 \pm 2r)]^{-1}$ are the eigenvalues of the effective mass tensor.⁵⁷ Here and below, we choose units such that \hbar and the lattice spacings are set equal to unity.

For $\varepsilon_{\perp} \leq \varepsilon \leq \varepsilon_{\top}$, the density of states $\nu(\varepsilon) = \oint_{\varepsilon_{\mathbf{k}}=\varepsilon} d\Omega_{\mathbf{k}} |\nabla_{\mathbf{k}} \varepsilon_{\mathbf{k}}|^{-1}$ can be computed analytically as⁵⁸

$$\nu(\varepsilon) = \frac{1}{\pi^2} \frac{1}{\sqrt{4t^2 - \varepsilon_c \varepsilon}} K \left[\frac{1}{2} \sqrt{\frac{16t^2 - (\varepsilon + \varepsilon_c)^2}{4t^2 - \varepsilon_c \varepsilon}} \right], \quad (3)$$

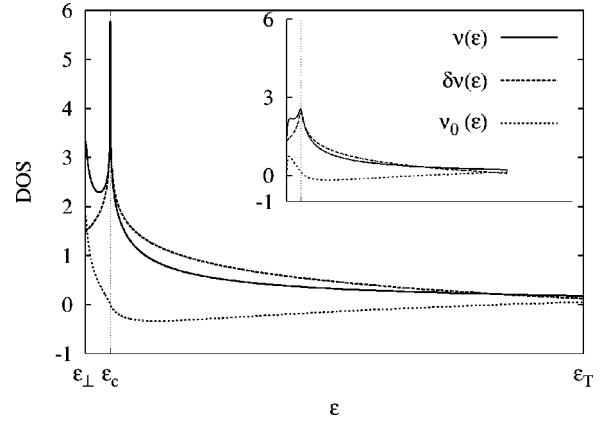


FIG. 2. Total density of states (ν), Eq. (3), and regular (ν_0) and singular ($\delta\nu$) contributions to the DOS, Eq. (4), as a function of energy ε , ranging from the bottom (ε_{\perp}) to the top (ε_{\top}) of the band. The inset shows the effect of a non-zero energy broadening Γ (here, $\Gamma \sim 0.5\%$ of the total bandwidth) on the same quantities [see Eq. (13)].

where $K(k)$ denotes the complete elliptic integral of first kind of modulus k (Ref. 59). At $\varepsilon = \varepsilon_c$, $\nu(\varepsilon)$ diverges logarithmically. Making use of the appropriate asymptotic expansion for $K(k)$ (Ref. 60), it is then customary to identify a regular and a singular contribution to $\nu(\varepsilon)$ as

$$\nu(\varepsilon) = \nu_0(\varepsilon) + \delta\nu(\varepsilon), \quad (4)$$

with $\nu_0(\varepsilon)$ being a continuous function of ε over the whole bandwidth such that $\nu_0(\varepsilon_c) = 0$, and

$$\delta\nu(\varepsilon) = 2\rho \ln \left| \frac{4\sqrt{2}/\pi^2 \rho}{\varepsilon - \varepsilon_c} \right|, \quad (5)$$

where $\rho^{-1} = 4\pi^2 t \sqrt{1-4r^2}$ (Fig. 2). In the following, we shall often make use of the critical parameter $z = \mu - \varepsilon_c$, measuring the distance of the chemical potential from the ETT.

III. THE EFFECT OF AN ETT ON THE SUPERCONDUCTING GAP

We will now discuss the effects of the proximity to an ETT on the superconducting properties of a 2D, single-layer system, both for an s - and d -wave order parameter, in the weak coupling limit. Our starting point will be the BCS equation for the gap function $\Delta_{\mathbf{k}}$, which at $T=0$ reads

$$\Delta_{\mathbf{k}} = -\frac{1}{N} \sum_{\mathbf{k}'} V_{\mathbf{k}\mathbf{k}'} \frac{\Delta_{\mathbf{k}'}}{2E_{\mathbf{k}'}}. \quad (6)$$

Here, $E_{\mathbf{k}} = \sqrt{\varepsilon_{\mathbf{k}}^2 + |\Delta_{\mathbf{k}}|^2}$ is the upper branch of the superconducting excitation spectrum, $V_{\mathbf{k}\mathbf{k}'}$ denotes the interparticle potential, and the sum runs over all the N \mathbf{k} points in the 1BZ. In the case of s -wave symmetry, we assume $V_{\mathbf{k}\mathbf{k}'} = -\lambda$, i.e., a constant over the whole 1BZ, whereas in the d -wave case we take the potential in the separable form $V_{\mathbf{k}\mathbf{k}'} = -\lambda g_{\mathbf{k}} g_{\mathbf{k}'}$, $g_{\mathbf{k}} = \frac{1}{2}(\cos k_x - \cos k_y)$ being the lowest-order lattice harmonic corresponding to d -wave symmetry.

Accordingly, one has $\Delta_{\mathbf{k}} = \Delta_0$ in the *s*-wave case, and $\Delta_{\mathbf{k}} = \Delta_0 g_{\mathbf{k}}$ in the *d*-wave case, respectively. It is worth emphasizing that, in both cases, the coupling constant $\lambda > 0$ has been assumed independent of doping. This amounts to neglecting higher-order correlation effects among interacting particles.⁴¹ Moreover, the weak coupling hypothesis allows us to neglect renormalizations of the shape of the Fermi surface, which are certainly expected in the strong coupling limit, and are known to give rise to another kind of ETT as well.⁶¹

Equation (6) implicitly neglects the possibility of any pairing instability other than singlet superconductivity in the Cooper channel (characterized by a pair relative momentum $\mathbf{P} = 0$). Possible alternative intervening pairing instabilities include, e.g., antiferromagnetism and the π -triplet paired state.³⁰ Such instabilities would be characterized by large momentum transfer near the “hot spots” $(0, \pi)$ and $(\pi, 0)$. They have been shown to coexist and win out singlet superconductivity at a mean field level near half-filling, when backward scattering is a relevant process.³⁰ However, within our weak-coupling approximation, it is consistent to retain only one kind of instability (namely, Cooper pairing in the singlet, $\mathbf{P} = 0$ channel, with either *s*- or *d*-wave symmetry), under the assumption that other instabilities are characterized by weaker couplings.

We will first analyze the gap equation, Eq. (6), close to an ETT ($|z| \ll 4t$). In the *s*-wave case, the summation over the 1BZ in Eq. (6) can be transformed into an integral over energy weighted by the DOS, which we approximate by its singular part $\delta\nu(\varepsilon)$ in Eq. (4). The Fermi line corresponding to the ETT divides the 1BZ in two regions, $\varepsilon_{\mathbf{k}} < 0$ and $\varepsilon_{\mathbf{k}} > 0$, which are electron-hole conjugated of each other. Separating the contributions coming from these regions, the gap equation can be compactly written as

$$\frac{1}{\lambda\rho} = S_+ + S_-, \quad (7)$$

where S_{\pm} represent the pairing susceptibility integrated between the ETT and either band edges (see Appendix A for details).

While in 3D BCS theory S_{\pm} are logarithmically divergent in the limit $\Delta_0 \rightarrow 0$ (Ref. 62), the proximity to an ETT in 2D makes them divergent as $\sim \ln^2 \Delta_0$. Direct inspection of Eq. (7) as well as numerical calculations show that $\Delta_0(z)$ is maximum near the ETT. Such a nonmonotonic dependence of the superconducting gap on the critical parameter z is in agreement with the phenomenology of the HTSC, where Δ_0 and T_c are characterized by a parabolalike dependence on doping.¹⁶ This has to be contrasted with the steplike behavior observed in the 3D case,¹⁸ where it has to be emphasized that no divergence occurs in the DOS at the ETT. However, due to the electron-hole symmetry breaking induced by a non-zero hopping ratio r , $\Delta_0(z)$ is not an even function of z , and its maximum will actually occur not exactly at $z = 0$, as will be discussed below. Solving Eq. (7) for Δ_0 in the weak-coupling limit ($\lambda\rho \ll 1$, $\Delta_0 \ll 4t$), at $z = 0$ one finds

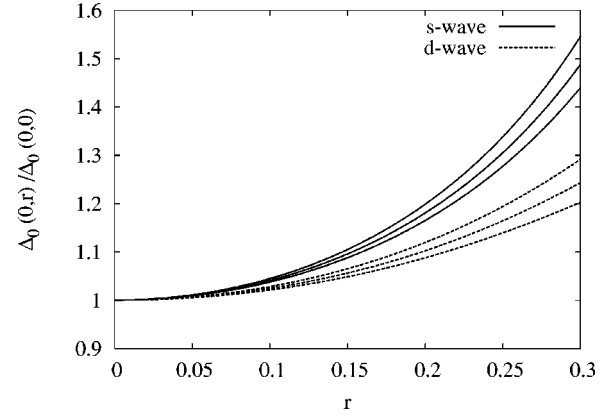


FIG. 3. Normalized gap amplitude $\Delta_0(z=0, r)/\Delta_0(z=0, r=0)$ at $T=0$, as a function of the hopping ratio $r = t'/t$, for different couplings $\lambda/t = 0.9-1.1$ (bottom to top). Continuous lines refer to the *s*-wave case, Eq. (8), while dashed lines refer to the *d*-wave case, Eq. (9). One can recognize the direct correlation between $T_c^{\max} \propto \Delta_0(z=0)$ and r , as observed in Ref. 39.

$$\Delta_0(z=0) \simeq \frac{8\sqrt{2}}{\pi^2\rho} \exp\left(-\sqrt{\frac{1}{\lambda\rho} + \frac{1}{4}\ln^2\frac{1+2r}{1-2r}}\right), \quad (\textit{s wave}) \quad (8)$$

which can be then taken as a first approximation to the gap maximum at $T=0$, in the *s*-wave case. Following the same procedure, qualitatively similar results can be derived for the critical temperature T_c as a function of z (see also Refs. 7,15).

In the *d*-wave case, due to the anisotropic \mathbf{k} dependence of the integrand in Eq. (6), it is not possible to explicitly separate the integration over energy, and a different approach must be followed (see Appendix A for details). However, the proximity to an ETT does endow the pairing susceptibility with an analogous asymptotic low- Δ_0 behavior, as in the *s*-wave case, which eventually results in the following weak-coupling expression for the gap amplitude at $T=0$, $z=0$ ($\lambda\rho \ll 1$, $\Delta_0 \ll 4t$):

$$\Delta_0(z=0) \simeq 4t f_1(r) \exp\left(-\sqrt{\frac{1}{\lambda\rho} + f_2(r)}\right), \quad (\textit{d wave}), \quad (9)$$

where $f_1(r) = 2b^{-1}(1-4r^2)(\sqrt{1+2r} + \sqrt{1-2r})^{-1}$, $f_2(r) = \ln^2(b\pi\sqrt{1-4r^2}) + 2\ln\sqrt{1-4r^2}\ln[2\pi^{-1}\sqrt{1-4r^2}(\sqrt{1+2r} + \sqrt{1-2r})^{-1}]$, and $b = e^2/8$.

Figure 3 shows $\Delta_0(0)$ both in the *s*- and in the *d*-wave case, Eqs. (8) and (9), respectively, as a function of the hopping ratio r , for several values of λ/t . In view of the fact that $T_c \propto \Delta_0$, as in any mean-field theory, Fig. 3 is in good qualitative agreement with Fig. 5 of Ref. 39, showing a direct correlation between the experimental T_c^{\max} and the hopping range r for several cuprate compounds. Moreover, our results suggest that such an effect is a general consequence of the proximity to an ETT, and is roughly independent of the superconducting pairing symmetry.

Expanding $\Delta_0(z)$, as implicitly defined by Eq. (7) around $z=0$, one finds that the maximum of Δ_0 actually occurs at a larger value of the critical parameter, which, in the s -wave case, is given by

$$z_{\max} \simeq \frac{1}{8t} \Delta_0^2(0) \ln \frac{1+2r}{1-2r}. \quad (10)$$

A qualitatively analogous result applies to the d -wave case. Therefore, as an effect of the electron-hole asymmetry induced by a nonzero hopping ratio r , the maximum in Δ_0 is actually located in the holelike region ($z_{\max} > 0$), in agreement with the phenomenology of some hole-doped cuprate compounds. For instance, a representative high- T_c cuprate such as LSCO is characterized by an optimal doping level of $x_{\text{opt}} \simeq 0.15$, lying in the hole-doped region, while a doping-dependent crossover from a holelike to an electronlike FS has been clearly observed at a somewhat larger doping $x_c \simeq 0.20$ (Ref. 6). On the contrary, no direct evidence of a change in the FS topology has been so far reported for Bi-2212 (Ref. 63), whose FS displays a holelike character at all dopings, including optimal doping. This implies that the ETT is located at a much larger distance from optimal doping, which is consistent with Eq. (10) above, given the larger value of the gap amplitude of Bi-2212 than that of LSCO.

IV. EFFECT OF IMPURITIES

We now turn to consider the more realistic case, in which electron scattering from nonmagnetic impurities is included. Here, we will be mainly concerned with the normal state properties. A finite quasiparticle lifetime induces a broadening of the energy linewidth of a quasiparticle state. Therefore, the use of a quasiparticle description and the definition of a Fermi surface for impure metals can, at first sight, be objected. Indeed, quasimomentum is a “good” quantum number only for electrons moving in a periodic potential.⁶⁴ Scattering of electrons on impurities results in momentum relaxation and in the corresponding smearing of the Fermi surface in momentum space. The characteristic scale of such a smearing is $\sim \tau^{-1}$, where τ is the elastic relaxation time at low temperatures. The value of τ can easily exceed the quasiparticle energy $\sim T$ even for moderate impurity concentrations.

Nevertheless, elastic scattering does not result in energy relaxation. This means that, in principle, one can solve exactly the eigenvalue problem for the Hamiltonian of the electron in a lattice with some specific realization of the impurity potential. The eigenstates of such Hamiltonian can then be chosen as a basis in the Hilbert space and the “Fermi surface” in this space can be defined as the surface separating the low-energy occupied eigenstates from the high-energy empty eigenstates at zero temperature. It is evident that the Fermi surface defined in this way does exist, and that the elastic scattering has no effect on the quasiparticle lifetime in the vicinity of the Fermi surface (see also Refs. 9,12).

The effect of a nonvanishing impurity scattering rate can then be accounted for in the DOS by means of a convolution between $\nu(\varepsilon)$ and a Lorentzian of finite width Γ :

$$\nu_{\Gamma}(\varepsilon) = \int d\xi \frac{1}{\pi} \frac{\Gamma}{(\xi - \varepsilon)^2 + \Gamma^2} \nu(\xi). \quad (11)$$

Such a procedure¹² effectively smears out the logarithmic singularity in the DOS at the ETT into a pronounced maximum of finite width $\sim \Gamma$ (see inset in Fig. 2). Nonetheless, it is still possible to separate a “regular” and a “singular” contribution to $\nu_{\Gamma}(\varepsilon)$ as

$$\nu_{\Gamma}(\varepsilon) = \nu_{\Gamma}^0(\varepsilon) + \delta\nu_{\Gamma}(\varepsilon), \quad (12)$$

with $\delta\nu_{\Gamma}(\varepsilon)$ now given by¹²

$$\delta\nu_{\Gamma}(\varepsilon) = 2\rho \ln \frac{4\sqrt{2}/\pi^2\rho}{\sqrt{(\varepsilon - \varepsilon_c)^2 + \Gamma^2}}. \quad (13)$$

From a physical point of view, the energy linewidth broadening associated to impurity scattering has the effect of “blurring” the Fermi line. As a consequence, one expects that the ETT occurs slightly farther from $\mu = \varepsilon_c$ (i.e., for $|z| > 0$), as soon as such a blurred Fermi line touches the border of the 1BZ.⁹

Thus far, we have assumed a constant energy linewidth Γ over the whole band. This is clearly an approximation, since the quasiparticle lifetime $\tau_{\mathbf{k}}$ is generally an anisotropic quantity over the 1BZ.⁶⁵ The last statement holds true even in the simplest case of isotropic impurity scattering, due to the anisotropy of the single-particle band structure. In particular, the proximity to an ETT in 2D endows the quasiparticle lifetime with a nonmonotonic behavior, in contrast to the 3D case, where a steplike z dependence was found.⁹ Following Ref. 9, one can write the self-consistent equation for the retarded quasiparticle self-energy Σ^R due to impurity scattering as

$$\Sigma^R(\omega, z) = \frac{n_i |u_0|^2}{(2\pi)^2} \int d^2\mathbf{p} [\epsilon_{\mathbf{p}} + z + \omega - \Sigma^R(\omega, z)]^{-1}, \quad (14)$$

where $\epsilon_{\mathbf{p}}$ is the asymptotic single-particle dispersion relation near the saddle point defining the ETT, Eq. (2), n_i denotes the concentration of impurities, and u_0 is the impurity scattering strength, here assumed independent of \mathbf{p} . Performing the integrations as in Refs. 9,66, but now for the 2D case, one arrives at the self-consistent expression

$$\Sigma^R = -\frac{i}{2\tau_0} \ln \left(\frac{\sqrt{1+z} + \sqrt{1+\omega + \Sigma^R}}{\sqrt{-\omega - z + \Sigma^R}} \right), \quad (15)$$

where $\tau_0^{-1} = \pi^{-1} n_i |u_0|^2 (m_1 m_2)^{1/2}$, and all energies are in units of a cut-off energy $\sim \rho^{-1}$. Figure 4 shows the renormalized quasiparticle inverse lifetime $\tau^{-1} = -2\text{Im}\Sigma^R(\omega = 0, z)$ as a function of the critical parameter z , for several values of τ_0^{-1} . As anticipated, one observes a maximum in τ^{-1} at $z \geq 0$, as an effect of crossing an ETT.

The study of a 2D superconductor in the dirty limit goes beyond the reach of the present analysis. The dependence of Δ_0 as well as of the DOS on the impurity concentration has been derived in the d -wave case in Ref. 67, for an isotropic

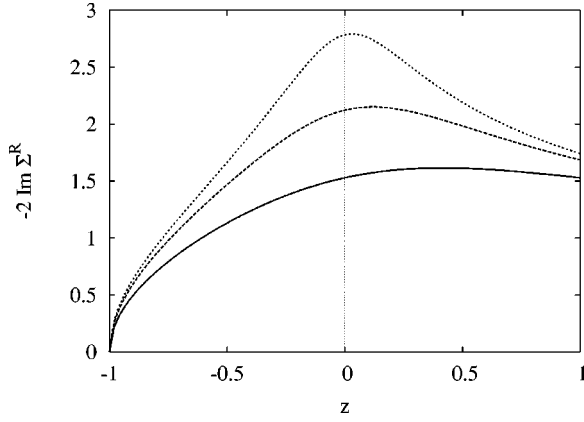


FIG. 4. Renormalized quasiparticle inverse lifetime $\tau^{-1} = -2\text{Im}\Sigma^R$, Eq. (15), resulting from isotropic impurity scattering. Different curves correspond to increasing values of τ_0^{-1} (bottom to top). The proximity to an ETT induces a nonmonotonic dependence of τ^{-1} on the critical parameter z , with τ^{-1} assuming its maximum value at $z \approx 0$.

dispersion relation. In d -wave superconductors, Dirac-like single-particle excitations can be created at virtually no energy cost near the gap nodes.^{68–70} Within the QCP scenario, long-range interaction between such gapless modes is mediated via the fluctuations of an intervening order parameter at $T=0$. Current proposals for the HTSC include the possibility of the proximity to a quantum ordered phase characterized by either charge or (AFM) spin fluctuations, as well as fluctuations related to the opening of another subdominant contribution to the superconducting OP, usually accompanied by time-reversal breaking.^{24,25} Recent results for 2D d -wave superconductors in the presence of disorder yield corrections to the density of states coming both from the diffusion ($\mathbf{Q}=0$) and the Cooperon mode,⁷¹ as well as from the diffusive mode with $\mathbf{Q}=(\pi, \pi)$.⁷²

V. GINZBURG-LANDAU STIFFNESS NEAR AN ETT

As is well known, the normal state of HTSC is characterized by several anomalous properties at the transition edge. Such properties include a peak in the c -axis resistivity, an anomalously large sign-changing c -axis magnetoresistance, as well as the opening of a pseudogap, which is observed both in the c -axis optical conductivity, in tunneling experiments, and in the NMR relaxation rate (see Ref. 40 for a review). On the basis of the Fermi liquid theory, it has been recently demonstrated that the renormalization of the one-electron DOS in the vicinity of the Fermi level due to the electron-electron interaction in the Cooper channel is able to explain satisfactorily many of these pseudogaplike manifestations both in the overdoped and in the optimally doped compounds.⁴⁰ Moving across the phase diagram of the HTSC from the overdoped, bad metallic region, towards underdoping, the enhancement of the mentioned effects correlates with an increase of the Ginzburg-Levanyuk parameter $\text{Gi}_{(2D)} \approx T_c/E_F$, thus making perturbation theory less reliable.⁴⁰ Nevertheless, such a rapid growth of the normal state anomalies with the decrease of doping strongly over-

comes the theoretical predictions, thus making it difficult to attribute such an effect to the mere shrinking of the FS.

Indeed, ARPES studies indicate a marked increase of the FS anisotropy in the ab plane with underdoping, which is accompanied by the development of an extended saddle point in the electronic spectrum.⁴³ One can identify two characteristic energy scales related with such a FS, namely the size of its “bulk” part $E_F \approx 0.3$ eV and the “width” of the saddle point $|z| = |\mu - \epsilon_c| \approx 0.01$ eV. The large difference in the magnitude of such energy scales is therefore suggestive of a crossover, related to the special role played by the electronic states lying close to the saddle point (the so-called “slow” electrons). Intuitively, one may expect a replacement of E_F with a small z in the denominator of $\text{Gi}_{(2D)}$, which would result in the breakdown of the perturbative approach developed in Ref. 40. Nevertheless, as is demonstrated below, the sole existence of an ETT in the electronic spectrum is not able to change the character of the isotropic electron-electron interaction in the Cooper channel. This implies that the breakdown of fluctuation theory in the underdoped compounds has to be related to some other properties of the HTSC. In order to substantiate the above statements, in the present section we shall derive the momentum dependence of the two-particle Green function in the Cooper channel near T_c and close to an ETT.

In the case of a 2D electron system characterized by the approximate spectrum given by Eq. (2), close to an ETT, the single-particle Green function can be written as

$$G(\mathbf{p}, \omega_n; z) = (i\omega_n - \epsilon_{\mathbf{p}} + z)^{-1}. \quad (16)$$

Here, the electron quasimomentum \mathbf{p} is measured from the saddle point location, as in Eq. (2), and $\omega_n = 2\pi T(n + \frac{1}{2})$ are the fermionic Matsubara frequencies. As already emphasized in Sec. II, the condition $z > 0$ describes the case of an open Fermi surface without any disrupted neck, whereas the opposite one, $z < 0$, is appropriate to a closed Fermi surface with respect to the Γ point (Fig. 1). The two-particle Green function in the Cooper channel $L(\mathbf{q}, \Omega_\nu)$ can be expressed within the ladder approximation by means of the polarization operator $\Pi(\mathbf{q}, \Omega_\nu)$ as⁴⁰

$$L^{-1}(\mathbf{q}, \Omega_\nu; z, T) = \lambda^{-1} - \Pi(\mathbf{q}, \Omega_\nu; z, T). \quad (17)$$

Here, $\lambda > 0$ denotes the momentum independent effective electron-electron interaction, \mathbf{q} is the Cooper pair momentum, and

$$\begin{aligned} \Pi(\mathbf{q}, \Omega_\nu; z, T) &= T \sum_{\omega_n} \int \frac{d^2\mathbf{p}}{(2\pi)^2} G(\mathbf{p} + \mathbf{q}, \omega_{n+\nu}; z) G(-\mathbf{p}, -\omega_n; z) \\ &\equiv T \sum_{\omega_n} I(\mathbf{q}, \omega_{n+\nu}, -\omega_n; z), \end{aligned} \quad (18)$$

with $\Omega_\nu = 2\pi T\nu$ the bosonic Matsubara frequencies.

The superconducting critical temperature can be characterized as the temperature at which L presents a pole at $\mathbf{q} = 0$ and $\Omega_\nu = 0$. The procedure to deal with the integral in Eq. (18) is outlined in Appendix B. One eventually arrives at the result

$$\Pi(0,0;z,T) = \frac{m}{\pi} T \sum_{\omega_n \geq 0}^{\omega_D/(2\pi T)} \frac{1}{\omega_n} \ln \left(\frac{\omega_D^2}{\omega_n^2 + z^2} \right), \quad (19)$$

where $m = \sqrt{m_1 m_2}$ is the geometric average mass around the saddle point, and the Debye frequency ω_D has been introduced as a cutoff in the summation over the Matsubara frequencies. The equation for the critical temperature then reads

$$\lambda^{-1} = \frac{m}{\pi} T_c \sum_{\omega_n \geq 0}^{\omega_D/(2\pi T_c)} \frac{1}{\omega_n} \ln \left(\frac{\omega_D^2}{\omega_n^2 + z^2} \right). \quad (20)$$

For small z ($|z| \ll \omega_D$), one recovers the well-known result⁴⁴

$$T_c \sim \frac{\omega_D}{2\pi} \exp \left(-\frac{1}{\sqrt{\lambda\rho}} \right), \quad (21)$$

where $\rho = m/(2\pi^2)$ denotes the DOS at the saddle point. Equation (21) is in agreement with the s -wave result for Δ_0 , Eq. (8), when the assumption of a phonon-mediated pairing mechanism is made and the limit $r \rightarrow 0$ is taken. Vertex and cross corrections to Eq. (21) in terms of the Migdal adiabaticity parameter ω_D/E_F have been shown to decrease the enhancement of T_c due to the proximity to an ETT.^{73,74} Analogously, for the two-particle Green function close to the superconducting transition and in the proximity of an ETT ($|z| \ll T \sim T_c$), one finds

$$L^{-1}(0,0;z,T) = -\rho \ln \left(\frac{\omega_D}{2\pi T_c} \right) \frac{T - T_c}{T_c}. \quad (22)$$

One observes that the presence of the ETT results in the appearance of the additional large factor $\sim \ln(\omega_D/T_c)$ in front of the reduced temperature.

In order to determine the superconducting stiffness tensor $\eta_i(z)$, one is led to consider the \mathbf{q} dependence of the polarization operator, Eq. (18). Expanding $I(\mathbf{q}, \omega_n, -\omega_n; z)$ in Eq. (18) for small q and z , up to quadratic order in q , one has

$$I(\mathbf{q}, \omega_n, -\omega_n; z) = I_0(0, \omega_n, -\omega_n; z) + I_1(q^2, \omega_n, -\omega_n; 0) + I_2(q^2, \omega_n, -\omega_n; z), \quad (23)$$

where I_j are defined in Appendix B, and I_0 has been used above for the definition of the critical temperature, Eq. (19). One eventually finds for the q^2 -dependence of the two-particle Green function in the limit $|z| \ll T \sim T_c$ the relatively classical form

$$L^{-1}(\mathbf{q}, 0; 0, T) = -\rho \left[\ln \left(\frac{\omega_D}{2\pi T_c} \right) \frac{T - T_c}{T_c} + \eta_1 q_1^2 + \eta_2 q_2^2 \right], \quad (24)$$

where the components of the superfluid stiffness tensor are given by

$$\eta_i(z) = \frac{7\zeta(3)E_F}{8\pi^2 T^2 m_i}, \quad (25)$$

to the lowest order in z/E_F . The latter expression is analogous to the result obtained in the standard 2D isotropic case, with $\xi_p = p^2/(2m) - \mu$, where the superfluid stiffness reads $\eta = 7\zeta(3)E_F/(16\pi^2 T^2 m)$, and the DOS per spin is $\rho_{(2D)} = m/(2\pi)$ (Ref. 9). It is worth noting that in Eq. (24) the effective mass of the fluctuating Cooper pair gets increased by a factor $\ln(\omega_D/2\pi T_c)$, with respect to the case in which a parabolic spectrum is assumed. This implies a reduced role of fluctuations near an ETT. Indeed, our results demonstrate that the temperature range of the fluctuation regime is governed by essentially the same G_i , while the propagator's effective mass is enhanced.

Summarizing, the results obtained above shows that a topological singularity in the electronic spectrum practically does not affect the Ginzburg-Landau stiffness, in contrast to what was intuitively speculated.⁴⁰ The reason thereof is that the value of η is formed by gathering the contributions of the electronic states belonging to the whole Fermi surface, not only by the “slow” ones. Finally, we note that in the approach we followed, only the polarization loop Eq. (18) is critical, since Cooper pairing of nonzero center-of-mass momentum is not taken into account.⁶²

VI. CONCLUSIONS

We have reviewed the effects of an electronic topological transition on the superconducting properties of a 2D electron system, with an energy spectrum characterized by a minimum at the Γ point and an extended, doping dependent saddle point at $(\pi, 0)$, as is typical for most single-layered, hole-doped HTSC. We analytically derived the expressions for the superconducting gap Δ_0 at $T=0$ close to an ETT, both in the s -wave and in the d -wave case. In contrast to the 3D result,¹⁸ Δ_0 turns out to be characterized by a nonmonotonic behavior as a function of the critical parameter z , with a maximum at $z \approx 0$, i.e., close to the ETT. Due to the electron-hole symmetry-breaking induced by a nonzero value of the hopping ratio r , we find that the maximum of Δ_0 actually occurs at $z \geq 0$, i.e., it is slightly shifted towards the holelike region, as observed in LSCO.⁶ We point out that in previous calculations^{15,19–21,28} the maximum of T_c as a function of the critical parameter z occurs at the ETT, $z=0$. This result has been often used as an objection against the relevance of the van Hove scenario for the cuprates, since ARPES data show that the optimal doping does not correspond to the critical point $z=0$, and that the FS preserves a holelike character over the entire doping range for almost all hole-doped compounds (see, however, also the recent results of Ino *et al.* for the LSCO compound⁶). On the contrary, we have shown that the observed difference between optimal doping and the doping actually corresponding to the ETT can be justified by taking into account an electronic spectrum beyond the hyperbolic approximation. Moreover, we find

that the dependence of Δ_0 on the hopping ratio r is in good qualitative agreement with the phenomenological results collected by Pavarini *et al.* for several HTSC materials,³⁹ thus demonstrating the role of the band structure peculiarities and, in particular, of next-nearest-neighbor hopping, in stabilizing high-temperature superconductivity in the cuprates.

In the presence of impurities, the Fermi line is effectively smeared, and one expects the anomalies due to the proximity to an ETT to occur at a larger value of the critical parameter, as soon as such a “blurred” Fermi line touches the zone border. We also derived the energy dependence of the retarded quasiparticle self-energy Σ^R due to impurity scattering in the 2D case, for a simplified, hyperbolic dispersion relation. In contrast to the 3D case, Σ^R is again characterized by a nonmonotonic z dependence, thus confirming that the quasiparticle lifetime $\tau_{\mathbf{k}}$ is generally an anisotropic quantity over the 1BZ.

Finally, we addressed the issue of the range of fluctuations near T_c . By explicitly computing the two-particle propagator in the Cooper channel near T_c , we derived the expression for the superfluid stiffness η close to an ETT. Although the Fermi velocity vanishes at the saddle point, we find a non-zero value of η , in complete analogy with the Ginzburg-Landau result for an isotropic electronic spectrum, thus showing that all electronic states participate in establishing the superconducting correlations. Moreover, our results show that the role of fluctuations even diminishes near the ETT. Indeed, while their temperature range is determined by about the same value of G_i , the effective mass of the fluctuating Cooper pair increases by a factor $\ln(\omega_D/2\pi T_c)$ with respect to the case of a parabolic spectrum. Therefore, in the denominator of any fluctuation contribution there appears a large logarithm, which implies a relative suppression of fluctuation effects near the ETT.

ACKNOWLEDGMENTS

We thank J. V. Alvarez, G. Balestrino, B. Ginatempo, F. Onufrieva, P. Pfeuty, P. Podio-Guidugli, R. Pucci, and G. Savona for useful discussions. Partial support from MURST through COFIN fund 2001 and the E.U. through the F.S.E. Program (G.G.N.A. and E.P.), and from I.N.F.M. and I.S.I. (Torino) through the “Progetto Stage” (G.G.N.A.) is gratefully acknowledged. G.G.N.A. also acknowledges the D.S.T.F.E. “Tor Vergata” and P. G. Nicosia for warm hospitality during the period in which the present work was brought to completion.

APPENDIX A: EVALUATION OF THE PAIRING SUSCEPTIBILITY IN THE d -WAVE CASE

We briefly outline the derivation of the asymptotic dependence of the integrated pairing susceptibility close to an ETT in 2D. In the s -wave case, changing integration variables in the gap equation, Eq. (6), from wave vector \mathbf{k} to energy, we can write the pairing susceptibility integrated between the ETT and either band edges as

$$S_{\pm} = - \int_0^1 \frac{\ln(a_{\pm}\xi)d\xi}{\sqrt{(\xi \mp \zeta_{\pm})^2 + \delta_{\pm}^2}}, \quad (\text{A1})$$

where we have introduced the dimensionless auxiliary quantities $\zeta_{\pm} = z/(4t \pm 8t')$, $\delta_{\pm} = \Delta_0/(4t \pm 8t')$, and $a_{\pm} = (1 \pm 2r)/(4\sqrt{2}\sqrt{1-4r^2})$.

In the d -wave case, the double integration over wave vector \mathbf{k} cannot be reduced to a simple integration over energy, and one has to change variables to $\xi = \pm(\varepsilon_{\mathbf{k}} - \varepsilon_c)/[4t(1 \pm 2r)]$, $g = g_{\mathbf{k}}$. In such a case, Eq. (6) can be written as

$$\frac{\pi^2 t}{2\lambda} = D_+ + D_-, \quad (\text{A2})$$

where the integrated pairing susceptibility now reads

$$D_{\pm} = \frac{1}{4} \int_0^1 d\xi \int_0^{1-\xi} dg \frac{g^2}{\sqrt{(\xi \mp \zeta_{\pm})^2 + \delta_{\pm}^2 g^2}} \frac{1}{\sqrt{J_1 J_2 J_3}}, \quad (\text{A3})$$

and

$$J_1 = (1 - 2rg)^2 + 4r[g - r + (1 \pm 2r)\xi], \quad (\text{A4a})$$

$$J_2 = (1 + g)^2 - (1 - \sqrt{J_1})^2/(4r^2), \quad (\text{A4b})$$

$$J_3 = (1 - g)^2 - (1 - \sqrt{J_1})^2/(4r^2). \quad (\text{A4c})$$

Equation (A3) leads to hyperelliptic integrals, that cannot be generally expressed in terms of known special functions.⁷⁵ We next set $\Omega = -(1 - \sqrt{J_1})/(2r)$, with $\Omega \rightarrow \xi$ as $r \rightarrow 0$, with which D_+ in Eq. (A3) transforms into

$$D_+ = \frac{1}{4} \int d\Omega \int dg \frac{g^2}{\sqrt{[r(v^2 - g^2) - z]^2 + \Delta_0^2 g^2}} \times \frac{1}{\sqrt{[(1 + \Omega)^2 - g^2][(1 - \Omega)^2 - g^2]}}, \quad (\text{A5})$$

where all energies are in units of $4t$ and the integration is to be performed over the curvilinear triangle defined by $g \geq 0$, $g \leq 1 - \Omega$, and $v^2 - g^2 \geq 0$, with $v^2 = 1 + \Omega^2 + \Omega/r$. Such triangle represents the holelike region of the 1BZ, $\varepsilon_{\mathbf{k}} \geq \varepsilon_c$, in these new coordinates.

In the limit $r \rightarrow 0$, one branch of the hyperbola defined by $g = v$ reduces to the $\Omega = 0$ axis, and $r(v^2 - g^2) \rightarrow \Omega$. A further change to polar coordinates as $\Omega = \rho \cos \theta$, $g = \rho \sin \theta$ then allows one to exactly decouple the two integrations in Eq. (A5), the integration over ρ leading to elliptic integrals. Extracting the logarithmic divergence of these latter near $\theta = \pi/2$ (corresponding to the ETT, together with $\rho = 1$) yields the answer [see Eq. (A6) below, with $r = 0$].

In the case $r \neq 0$, we could not find any such simple change of variables, allowing to exactly decouple the integrations in Eq. (A5). However, since only the behavior of the dispersion relation close to the ETT is believed to determine the asymptotic properties of the integrated pairing suscepti-

bility, we may linearly expand $r(v^2 - g^2)$ near $\Omega = 0$, $g = 1$ and set $\Omega + 2r(g - 1) = \rho \cos \theta$. Within such approximation, Eq. (A5) then reads

$$D_+ = \frac{1}{4} \int_0^{\pi/2} d\theta \frac{\sin^2 \theta}{\sqrt{\cos^2 \theta + \Delta_0^2 \sin^2 \theta}} \times \frac{|\alpha_- \beta_+|}{1 - 4r^2} \\ \times \int_0^{\alpha_-} d\rho \frac{\rho^2}{\sqrt{(\alpha_+ + \rho)(\alpha_- - \rho)(\beta_+ + \rho)(\beta_- - \rho)}}, \quad (\text{A6})$$

where

$$\alpha_{\pm} = \frac{1 \pm 2r}{\cos \theta + (1 - 2r) \sin \theta}, \quad (\text{A7a})$$

$$\beta_{\pm} = \frac{1 \pm 2r}{\cos \theta - (1 + 2r) \sin \theta}. \quad (\text{A7b})$$

Following standard methods (see, e.g., Ref. 76), the inner integral can be now expressed as a combination of elliptic integrals, which diverge logarithmically as $\theta \rightarrow \pi/2$, whence Eq. (9) follows.

APPENDIX B:

EVALUATION OF THE POLARIZATION OPERATOR

The momentum integration in Eq. (18) for the polarization operator can be performed by reducing the integration domain to the first quarter of the 1BZ, and dividing the latter into the two triangles defined by $\{\mathbf{p}: p_2 \leq (m/m_1)p_1; p_1 \geq 0\}$ and $\{\mathbf{p}: p_2 \geq (m/m_1)p_1; p_1 \geq 0\}$, respectively. One finds

$$\Pi(0,0;z,T) = T \sum_{\omega_n} I(0, \omega_n, -\omega_n; z) \quad (\text{B1}) \\ = \frac{2m}{\pi^2} T \sum_{\omega_n} [f(\omega_n, -\omega_n; z) + f(\omega_n, -\omega_n; -z)], \quad (\text{B2})$$

where

$$f(\omega_n, -\omega_n; z) = \int_0^\infty dx_1 \int_0^x dx_2 \frac{1}{x_2^2 - x_1^2 - i\omega_n + z} \\ \times \frac{1}{x_2^2 - x_1^2 + i\omega_n + z}. \quad (\text{B3})$$

Performing the inner integration, one obtains

$$f(\omega_n, -\omega_n; z) = \frac{1}{2i\omega_n} \int_0^\infty dx \left[\frac{\ln(x - i\sqrt{z - i\omega_n - x^2})}{\sqrt{z - i\omega_n - x^2}} \right. \\ \left. - \frac{\ln(x + i\sqrt{z - i\omega_n - x^2})}{\sqrt{z - i\omega_n - x^2}} - \text{H.c.} \right]. \quad (\text{B4})$$

The last integration can be carried out observing that

$$\frac{\ln(x \pm i\sqrt{z - i\omega_n - x^2})}{\sqrt{z - i\omega_n - x^2}} = \pm \frac{i}{2} \frac{d}{dx} \ln^2(x \pm i\sqrt{z - i\omega_n - x^2}), \quad (\text{B5})$$

and choosing the branches of the logarithms in order to make them complex conjugated of each other. Finally, we obtain

$$I(0, \omega_n, -\omega_n; z) = \frac{m}{2\pi} \frac{1}{|\omega_n|} \ln \frac{\omega_D^2}{z^2 + \omega_n^2}. \quad (\text{B6})$$

In order to calculate the GL stiffness, let us now expand the polarization operator up to quadratic order in q . One has

$$\Pi(q, 0; z, T) = \Pi(0, 0; z, T) + \rho \sum_{i=1,2} \eta_i q_i^2, \quad (\text{B7})$$

where the components η_i of the stiffness tensor are defined by

$$\rho \sum_{i=1,2} \eta_i q_i^2 = T \sum_{\omega_n} [I_1(q^2, \omega_n, -\omega_n; 0) \\ + I_2(q^2, \omega_n, -\omega_n; z) + \dots]. \quad (\text{B8})$$

One explicitly finds

$$\eta_i(z) = \frac{1}{2m_i} T \sum_{\omega_n} \int \frac{d^2 \mathbf{x}}{x_2^2 - x_1^2 - i\omega_n} \frac{x_i^2}{(x_2^2 - x_1^2 + i\omega_n)^3} \\ - \frac{z}{2m_i} T \sum_{\omega_n} \int d^2 \mathbf{x} \sum_{k=0}^1 \frac{3^k}{(x_2^2 - x_1^2 + i\omega_n)^{3+k}} \\ \times \frac{x_i^2}{(x_2^2 - x_1^2 - i\omega_n)^{2-k}}$$

to the first order in z/E_F . The first integral, giving the principal contribution to the stiffness, can be evaluated using polar coordinates as

$$\eta_i(z=0) \\ = \frac{T}{m_i} \sum_{\omega_n} \frac{1}{\omega_n^2} \int_0^{2\pi} d\phi \int_0^\infty dr \frac{r^3 (r^4 \cos^2 2\phi - 1) \cos^2 \phi}{(r^4 \cos^2 2\phi + 1)^3} \\ = -\frac{\pi T}{4m_i} \sum_{\omega_n} \frac{1}{\omega_n^2} \int_0^\infty dt \left[\frac{\partial}{\partial \alpha} + \frac{\partial^2}{\partial \alpha^2} \right] \frac{1}{\sqrt{\alpha} \sqrt{t + \alpha}} \Big|_{\alpha=1} \\ \sim \frac{\pi T}{m_i} \sum_{n \geq 0} \frac{1}{\omega_n^3} E_F = \frac{7\zeta(3)E_F}{8\pi^2 T^2 m_i}. \quad (\text{B9})$$

- ¹P. W. Anderson, *The Theory of Superconductivity in the High- T_c Cuprates* (Princeton University Press, Princeton, NJ, 1997).
- ²D. G. Clarke and S. P. Strong, *Adv. Phys.* **46**, 545 (1997).
- ³Z.-X. Shen and D. S. Dessau, *Phys. Rep.* **253**, 1 (1995).
- ⁴R. H. McKenzie, *Science* **278**, 820 (1997).
- ⁵T. Yokoya, A. Chainani, T. Takahashi, H. Katayama-Yoshida, M. Kasai, and Y. Tokura, *Phys. Rev. Lett.* **76**, 3009 (1996); see also A. P. Mackenzie, S. R. Julian, G. G. Lonzarich, Y. Maeno, and T. Fujita, *ibid.* **78**, 2271 (1997); T. Yokoya, A. Chainani, T. Takahashi, H. Katayama-Yoshida, M. Kasai, and Y. Tokura, *ibid.* **78**, 2272 (1997).
- ⁶A. Ino, C. Kim, M. Nakamura, T. Yoshida, T. Mizokawa, Z.-W. Shen, A. Fujimori, T. Kakeshita, H. Eisaki, and S. Uchida, *Phys. Rev. B* **65**, 094504 (2002).
- ⁷R. S. Markiewicz, *J. Phys. Chem. Solids* **58**, 1179 (1997).
- ⁸The generic relevance of the Van Hove scenario for high- T_c superconductivity in the cuprates has been however questioned at least for the RBCO family [J. L. Tallon, G. V. M. Williams, C. Bernhard, D. M. Pooke, M. P. Staines, J. D. Johnson, and R. H. Meinhold, *Phys. Rev. B* **53**, R11 972 (1996)]. Yet another open issue is the competition of an ETT with an intervening structural instability, as exhibited by LSCO near optimal doping, and with the tendency exhibited by some layered cuprates to self-dope.
- ⁹A. A. Varlamov, V. S. Egorov, and A. V. Pantsulaya, *Adv. Phys.* **38**, 469 (1989).
- ¹⁰I. M. Lifshitz, *Zh. Éksp. Teor. Fiz.* **38**, 1569 (1960) [*Sov. Phys. JETP* **11**, 1130 (1960)].
- ¹¹S. Dorbolo, M. Ausloos, and M. Houssa, *Phys. Rev. B* **57**, 5401 (1998).
- ¹²Y. M. Blanter, M. I. Kaganov, A. V. Pantsulaya, and A. A. Varlamov, *Phys. Rep.* **245**, 159 (1994).
- ¹³E. Bruno, B. Ginatempo, E. S. Giuliano, A. V. Ruban, and Y. K. Velikov, *Phys. Rep.* **249**, 353 (1994).
- ¹⁴It should be noted that quantum critical fluctuations may give rise to a strong DOS renormalization, as has been shown in the case of a disordered electron system near a ferromagnetic quantum critical point at $T=0$ [D. Belitz, T. R. Kirkpatrick, R. Narayanan, and Th. Vojta, *Phys. Rev. Lett.* **85**, 4602 (2000)]. In the following, however, we shall neglect such effects, for the sake of simplicity.
- ¹⁵C. C. Tsuei, D. M. Newns, C. C. Chi, and P. C. Pattnaik, *Phys. Rev. Lett.* **65**, 2724 (1990).
- ¹⁶H. Zhang and H. Sato, *Phys. Rev. Lett.* **70**, 1697 (1993).
- ¹⁷R. J. Wijngaarden, D. T. Jover, and R. Griessen, *Physica B* **265**, 128 (1999).
- ¹⁸V. I. Makarov and V. G. Bar'yakhtar, *Zh. Éksp. Teor. Fiz.* **48**, 1717 (1965) [*Sov. Phys. JETP* **21**, 1151 (1965)].
- ¹⁹P. C. Pattnaik, C. L. Kane, D. M. Newns, and C. C. Tsuei, *Phys. Rev. B* **45**, 5714 (1992).
- ²⁰D. M. Newns, H. R. Krishnamurthy, P. C. Pattnaik, C. C. Tsuei, and C. L. Kane, *Phys. Rev. Lett.* **69**, 1264 (1992).
- ²¹D. M. Newns, C. C. Tsuei, and P. C. Pattnaik, *Phys. Rev. B* **52**, 13 611 (1992).
- ²²S. Gopalan, O. Gunnarsson, and O. K. Andersen, *Phys. Rev. B* **46**, 11 798 (1992).
- ²³I. Dzyaloshinskii, *J. Phys. I* **6**, 119 (1996).
- ²⁴S. Chakravarty, R. B. Laughlin, D. K. Morr, and C. Nayak, *Phys. Rev. B* **63**, 094503 (2001).
- ²⁵M. Vojta, Y. Zhang, and S. Sachdev, *Phys. Rev. Lett.* **85**, 4940 (2000).
- ²⁶F. Onufrieva, P. Pfeuty, and M. Kiselev, *Phys. Rev. Lett.* **82**, 2370 (1999).
- ²⁷F. Onufrieva and P. Pfeuty, *Phys. Rev. Lett.* **82**, 3136 (1999); **83**, 1271 (1999).
- ²⁸F. Onufrieva and P. Pfeuty, *Phys. Rev. B* **61**, 799 (2000).
- ²⁹F. Onufrieva, S. Petit, and Y. Sidis, *Phys. Rev. B* **54**, 12 464 (1996).
- ³⁰M. Murakami and H. Fukuyama, *J. Phys. Soc. Jpn.* **67**, 41 (1998).
- ³¹J. V. Alvarez, J. González, F. Guinea, and M. A. H. Vozmediano, *J. Phys. Soc. Jpn.* **67**, 1868 (1998).
- ³²J. González, F. Guinea, and M. A. H. Vozmediano, *Phys. Rev. Lett.* **84**, 4930 (2000).
- ³³J. V. Alvarez and J. González, *Europhys. Lett.* **44**, 641 (1998).
- ³⁴V. Irkhin, A. A. Katanin, and M. I. Katsnelson, *Phys. Rev. B* **64**, 165107 (2001).
- ³⁵M. Kiselev, F. Bouis, F. Onufrieva, and P. Pfeuty, *Eur. Phys. J. B* **16**, 601 (2000).
- ³⁶C. Honerkamp, M. Salmhofer, N. Furukawa, and T. M. Rice, *Phys. Rev. B* **63**, 035109 (2001).
- ³⁷N. Furukawa, T. M. Rice, and M. Salmhofer, *Phys. Rev. Lett.* **81**, 3195 (1998).
- ³⁸A. M. Gabovich, A. I. Voitenko, J. F. Annett, and M. Ausloos, *Semicond. Sci. Technol.* **14**, R1 (2001).
- ³⁹E. Pavarini, I. Dasgupta, T. Saha-Dasgupta, O. Jepsen, and O. K. Andersen, *Phys. Rev. Lett.* **87**, 047003 (2001).
- ⁴⁰A. A. Varlamov, G. Balestrino, E. Milani, and D. V. Livanov, *Adv. Phys.* **48**, 655 (1999).
- ⁴¹A. Perali, C. Castellani, C. Di Castro, M. Grilli, E. Piegari, and A. A. Varlamov, *Phys. Rev. B* **62**, R9295 (2000).
- ⁴²O. K. Andersen, A. I. Liechtenstein, O. Jepsen, and F. Paulsen, *J. Phys. Chem. Solids* **56**, 1573 (1995).
- ⁴³M. Randeria and J. Campuzano, in *Models and Phenomenology for Conventional and High-Temperature Superconductivity*, edited by G. Iadonisi, J. R. Schrieffer, and M. L. Chiofalo (IOS, Amsterdam, 1999), Proceedings of the CXXXVI International School of Physics "E. Fermi," Varenna (Italy), 1997.
- ⁴⁴A. A. Abrikosov, J. Campuzano, and K. Gofron, *Physica C* **214**, 73 (1993).
- ⁴⁵D. S. Dessau, Z.-X. Shen, D. M. King, D. S. Marshall, L. W. Lombardo, P. H. Dickinson, A. G. Loeser, J. DiCarlo, C.-H. Park, A. Kapitulnik, and W. E. Spicer, *Phys. Rev. Lett.* **71**, 2781 (1993).
- ⁴⁶K. Gofron, J. C. Campuzano, A. A. Abrikosov, M. Lindroos, A. Bansil, H. Ding, D. Koelling, and B. Dabrowski, *Phys. Rev. Lett.* **73**, 3302 (1994).
- ⁴⁷C. Hodges, H. Smith, and J. W. Wilkins, *Phys. Rev. B* **4**, 302 (1971).
- ⁴⁸A. J. Millis, H. Monien, and D. Pines, *Phys. Rev. B* **42**, 167 (1990).
- ⁴⁹V. J. Emery and S. A. Kivelson, *Nature (London)* **374**, 434 (1995).
- ⁵⁰C. Castellani, C. Di Castro, and M. Grilli, *Phys. Rev. Lett.* **75**, 4650 (1995).
- ⁵¹V. J. Emery and S. A. Kivelson, *Physica C* **209**, 597 (1993).
- ⁵²S. Chakravarty, A. Sudbø, P. W. Anderson, and S. Strong, *Science* **261**, 337 (1993).

- ⁵³G. G. N. Angilella, R. Pucci, F. Siringo, and A. Sudbø, Phys. Rev. B **59**, 1339 (1999).
- ⁵⁴J. González, F. Guinea, and M. A. H. Vozmediano, Europhys. Lett. **34**, 711 (1996).
- ⁵⁵J. González, Phys. Rev. B **63**, 045114 (2000).
- ⁵⁶V. Yu. Irkhin, A. A. Katanin, and M. I. Katsnelson, cond-mat/0110516 (unpublished).
- ⁵⁷Since the effective mass tensor is nondegenerate on every critical point of $\varepsilon_{\mathbf{k}}$, i.e., $\det \partial_{k_i k_j} \varepsilon_{\mathbf{k}} \neq 0$ when $\partial_{k_i} \varepsilon_{\mathbf{k}} = 0$, $\varepsilon_{\mathbf{k}}$ plays the role of a Morse function over the 1BZ [see, e.g., J. Milnor, *Morse Theory*, Ann. Math. Studies 51 (Princeton University Press, Princeton, 1963)].
- ⁵⁸D. Y. Xing, M. Liu, and C. D. Gong, Phys. Rev. B **44**, 12 525 (1991).
- ⁵⁹I. S. Gradshteyn and I. M. Ryzhik, *Table of Integrals, Series, and Products*, 5th ed. (Academic Press, Boston, 1994).
- ⁶⁰*Handbook of Mathematical Functions*, edited by M. Abramowitz and I. A. Stegun (Dover, New York, 1964).
- ⁶¹A. V. Chubukov and D. K. Morr, Phys. Rep. **288**, 355 (1997).
- ⁶²A. A. Abrikosov, L. P. Gorkov, and I. E. Dzyaloshinski, *Methods of Quantum Field Theory in Statistical Physics* (Dover, New York, 1975).
- ⁶³A. G. Loeser, D. S. Dessau, and Z. Shen, Physica C **263**, 208 (1996).
- ⁶⁴L. D. Landau and E. M. Lifshitz, *Physical Kinetics*, Vol. 10 of *Course of Theoretical Physics* (Pergamon, New York, 1981).
- ⁶⁵R. Hlubina and T. M. Rice, Phys. Rev. B **51**, 9253 (1995).
- ⁶⁶A. A. Varlamov and A. V. Pantsulaya, Zh. Éksp. Teor. Fiz. **89**, 2188 (1985) [Sov. Phys. JETP **62**, 1263 (1985)].
- ⁶⁷Y. Sun and K. Maki, Phys. Rev. B **51**, 6059 (1995).
- ⁶⁸P. A. Lee, Science **277**, 50 (1997).
- ⁶⁹P. A. Lee and X. G. Wen, Phys. Rev. Lett. **78**, 4111 (1997).
- ⁷⁰L. Balents, M. P. A. Fisher, and C. Nayak, Int. J. Mod. Phys. B **12**, 1033 (1998).
- ⁷¹D. V. Khveshchenko, A. G. Yashenkin, and I. V. Gornyi, Phys. Rev. Lett. **86**, 4668 (2001).
- ⁷²A. G. Yashenkin, W. A. Atkinson, I. V. Gornyi, P. J. Hirschfeld, and D. V. Khveshchenko, Phys. Rev. Lett. **86**, 5982 (2001).
- ⁷³E. Cappelluti and L. Pietronero, Phys. Rev. B **53**, 932 (1996).
- ⁷⁴E. Cappelluti and L. Pietronero, Europhys. Lett. **36**, 619 (1996).
- ⁷⁵M. Liu, D. Y. Xing, and Z. D. Wang, Phys. Rev. B **55**, 3181 (1997).
- ⁷⁶H. Hancock, *Lectures on the Theory of Elliptic Functions* (Wiley, New York, 1910), Vol. 1.